Bi-trophic food chain dynamics with multiple component populations

B.W. Kooi and P.P.F. Hanegraaf
Dept. of Theoretical Biology,
Institute of Ecological Science,
Faculty of Biology, Free University,
De Boelelaan 1087, 1081 HV Amsterdam,
The Netherlands

Bull. Math. Biol. **63: 271–299, 2001**

Abstract

Food web models describe the patterns of material and energy flow in communities. In classical food web models the state of each population is described by a single variable which represents, for instance, the biomass or number of individuals that make up the population. However, in a number of models proposed recently in the literature the individual organisms consist of two components. In addition to the structural component there is an internal pool of nutrients, lipids or reserves. Consequently the population model for each trophic level is described by two state variables instead of one. As a result the classical predator–prey interaction formalisms have to be revised. In our model time budgets with actions as searching and handling provide the formulation of the functional response for both components. In the model, assimilation of the ingested two prey components is done in parallel and the extracted energy is added to a predators reserve pool. The reserves are used for vital processes; growth, reproduction and maintenance. We will explore the top-down modelling approach where the perspective is from the community. We will demonstrate that this approach facilitates a check on the balance equations for mass and energy at this level of organisation. Here it will be shown that, if the individual is allowed to shrink when the energy reserves are in short to pay the maintenance costs, the growth process has to be 100% effective. This is unrealistic and some alternative model formulations are discussed. The long-term dynamics of a microbial food chain in the chemostat are studied using bifurcation analysis. The dilution rate and the concentration of nutrients in the reservoir are the bifurcation parameters. The studied microbial bi-trophic food chain with two-component population models shows chaotic behaviour.

1 Introduction

In classical food web models (Polis and Winemiller, 1996) populations consist of one component. In the past it was measured as amount of energy and at present often by number of individuals or biomass. To model predator–prey interactions different types of functional responses, for instance Lotka-Volterra (linear) or Holling (hyperbolic) functional response, are in common usage. Then, the consumption rate of the prey depends on the number of individuals or biomass density of the prey and the predator population.

The Monod model (Monod, 1942) is classical in the dynamics of populations consisting of unicellular microorganisms. In that model a fixed portion of the ingested nutrient is used for growth. The food ingestion rate is given by the Holling type II functional response. The model is called the Monod-Herbert model (Herbert, 1958) or the Marr-Pirt model (Pirt, 1965) when maintenance is introduced. Then a part of the ingested food is used for maintenance to keep the organism functioning, and the rest for growth.

In another variant of the Monod model, Droop (Droop, 1973) introduced the concept of cell nutrient quota (internal nutrient density) in addition to biomass in a model for phytoplankton growth. In this model growth is decoupled from nutrient uptake. It assumes that phytoplankton cells store nutrient and that the growth rate depends on the amount of stored nutrient. More recently models were proposed where two components in an organism are also distinguished. In (Hallam et al., 1990) a model is described where an organism consists of storage: lipids, the major source of energy, and a structural component: non-lipid dry material consisting mostly of proteins and carbohydrates. In (Persson et al., 1998) the components are called the reversible and irreversible mass. In reversible mass they include energy reserves such as fat, muscle tissue and gonads, and in irreversible mass they include compounds like bones and organs which cannot be starved away by the consumer. The Dynamic Energy Budget (DEB) model (Kooijman, 2000), deals with storage materials (reserves) and structural biomass. Here the storage materials are: carbohydrates, lipids but also a part of ribosomal RNA and of the proteins (Hanegraaf et al., 2000). The storage materials have a dual function as a reserve pool for energy and elementary compounds. These storage materials are continuously used and replenished, while structural materials are permanent and need maintenance.

The decomposition of organisms into two components implies that the predator–prey (trophic) interaction, as formulated in the classical food web models, has to be revised. The predators feed on prey that consist of two components with different composition. So, even when they are specialized on one single prey species they consume two nutrients. Holling type II (hyperbolic) functional response models for nutrient uptake rest on the mechanism that each arriving prey individual blocks the digestion apparatus of the predator for a certain period, see also (Kooijman, 2000). Prey individuals that arrive while the digestion apparatus is busy, are rejected. If the intensity of the arrival process is taken to be proportional to the prey density this mechanism ensures that the uptake rate is a hyperbolic function of the prey density. Following (Hanegraaf et al., 2000), where multiple nutrients are transferred into the organism by carriers, each component in parallel by its own assimilation pathway. When the transport of the reserve materials is faster than that

of structural materials the handling time is determined by the uptake and digestion of the structural biomass component of the prey individuals. So, the Holling type II functional response remains applicable.

In the DEB model there are three processes, assimilation, maintenance and growth. In this way we avoid a detailed description of the metabolic activity and the underlying biochemistry and physics. Thus, we skip over a wealth of biological detail. Food is converted into reserves, a process called assimilation, and the reserves are used for growth and maintenance. In these three processes chemical conversion occurs in exothermic reactions. Energy is lost as waste heat or in the form of chemical energy by the formation of waste products, see for instance (Roels, 1983). The process rates depend on the amounts of both individual components, namely the mass of the structural component and the reserve density, that is mass of reserves per structural mass, together with the density of the available food. Some relevant details of the model are presented in the Section 2 on the model for individuals.

In the individual-based modelling approach followed in this article, the model for the dynamics of the population is derived systematically from first principles where we start with the individual level using conservation laws for mass fluxes. Then we treat constitutive relationships which describe the coupling between mass and energy fluxes, together with environmental conditions, such as food availability. As a result the parameters in the population model have a meaning at the individual level. Generally, the resulting mathematical model at the population level is a set of partial differential equations (PDEs). Under simplifying assumptions a structured population dynamic PDE model describing them can be reduced to an equivalent unstructured ODE model, where the population model is derived by averaging over individuals.

In this paper we analyse the dynamics of a microbial bi-trophic community in the chemostat. The food chain consists of one nutrient, a prey population and a predator population which consumes the prey. In the bottom-up approach the community model is obtained by combining the population models and the description of their interaction in the chemostat reactor and their interaction with the environment. The parameter values for the vital rates are taken from (Nisbet et al., 1983) and are based on parameter estimations for microbial populations. In Section 4.1 the model resulting from the bottom-up approach, where modelling is done from the individual perspective, is given.

A top-down approach, where modelling is done from the community perspective, is worked out in Section 4.2. We check the community formulation with respect to conservation laws for mass and energy, and the second law of thermodynamics. This check resembles the use of dimensional analysis in checking mathematical relationships for the consistency of their dimensions. The top-down approach reveals that often hidden assumptions are made in the transition from individual to the community level. Here this approach will indicate that when shrinkage is allowed, the growth process has to be 100% effective, which means that there is neither heat production nor product formation. We will show that at this point individual-based modelling really makes a basic difference compared to the classical way of modelling where modelling is done from the population perspective (Uchmański and Grimm, 1996).

The material of this paper consists of a combination of interpretation of past work and new results. A set of conditions is derived for mass-energy coupling in the DEB model for individuals (Kooijman et al., 1999; Kooijman, 2000). We aim to analyse the long-term dynamics of a bi-trophic food chain using bifurcation analysis. The study of asymptotic dynamics of food chains in the chemostat (Kooi et al., 1998a; Kooi et al., 1999; Hanegraaf et al., 2000) is extended with predator-prey interactions where not only the structure but also the reserves of the prey are assimilated by the predator. In earlier work it was assumed implicitly that shrinking of structure was allowed (Kooi et al., 1998a; Kooi et al., 1999). Here we show that this assumption has theoretical consequences and a major impact on the bifurcation diagrams where the system shows oscillatory behaviour.

For the microbial bi-trophic food chain, with two component populations, where each population is described by two state variables, a period doubling route leads to chaotic behaviour. With one-component population models, and consequently one state variable for each population, no chaotic behaviour is observed when the parameter values and the ranges of the bifurcation parameters are the same.

2 Individual level

The system consists of the individual and its environment. The mass conservation law holds for chemical elements. In addition to elements chemical compounds are considered, because the particular composition of the elements in a chemical compound determines the energy content.

We assume that three chemical transformation processes take place in the individual; assimilation $\mathcal{A}$, maintenance $\mathcal{D}$ and growth $\mathcal{G}$ (see also Figure 1):

$$X_X \xrightarrow{\mathcal{A},\nu} X_E + X_A \ , \quad X_E \xrightarrow{\mathcal{D},m} X_D \ , \quad X_E \xrightarrow{\mathcal{G},g} X_V + X_G \ . \tag{1}$$

Reserve material, X_E, is generated from the nutrient, X_X, by the assimilation process. The energy stored in the reserve materials is used in the maintenance process and the growth process whereby structural material, X_V, is formed. Non-limiting nutrients are consumed in chemical processes and products are formed. In the mathematical description they differ only in sign. So, for each process, $\mathcal{P} \in \{\mathcal{A}, \mathcal{D}, \mathcal{G}\}$, we can combine these materials and call them "products". These combined products are denoted by X_A, X_D and X_G for the assimilation, maintenance and growth process, respectively. Although we do not give a precise definition, in biological applications it is clear what should be called products and what non-limiting nutrients. Thus, the reserve material, X_E and the structural material, X_V are part of the individual. The products, X_A, X_D and X_G, are materials that are taken up from or excreted in the environment.

Let $M_c(t)$ denote the mass of a compound in the individual and $J_c = dM_c/dt$, $c \in \{V, E\}$ the rate of change of this mass. The mass flux of the material exchanged with the environment is denoted by J_c, $c \in \{X, A, D, G\}$. Flux J_X is the limiting nutrient uptake flow. Fluxes J_A, J_D and J_G concern all products and non-limiting nutrients of the transformation assimilation, maintenance and growth.

The flux J_A concerns products and non-limiting nutrients in the assimilation process: faeces production or product formation by microorganisms, forms part of this flux. The flux J_G denotes products and nutrient associated with the synthesis of structure. Respiration, that is the use of oxygen or the production of carbon dioxide, is frequently identified with routine metabolic costs, conceived as maintenance costs. However, the flux J_D associated with the maintenance process, is here not exclusively linked to carbon dioxide and oxygen fluxes (Kooijman et al., 1999).

Usually, when a compound is consumed one has $J_c < 0$ and $J_c > 0$ when a compound is produced and excreted into the environment. Here products and non-limiting nutrients are represented by one net compound for each process. This is possible because the stoichiometry of each of these processes is invariant. So, a net compound can have positive but also negative chemical indices, whether there is a net production or a net consumption of the element.

Both reserves and structure are taken to be generalized compounds, that is, rich mixtures of chemical compounds that do not change in time. All elements occurring in the organism, $\mathrm{e} \in \{\mathrm{C}, \mathrm{H}, \mathrm{O}, \mathrm{N}, \cdots\}$, are taken into account. For each compound we have the molecular composition $\mathrm{C_1H}_{n_{\mathrm{H}c}}\mathrm{O}_{n_{\mathrm{O}c}}\mathrm{N}_{n_{\mathrm{N}c}}, \cdots$. Without loss of generality, we choose the chemical indices of the compounds for carbon equal to 1 and refer to their amounts as C-moles. For instance, in (Hanegraaf et al., 2000) parameter values for the elemental composition of the structural biomass, $\mathrm{C_1H_{1.564}O_{0.487}N_{0.206}}$, and that of the reserves, $\mathrm{C_1H_{1.393}O_{0.715}N_{0.181}}$ are estimated for the rumen bacterium *Selenomonas ruminantium*.

The elemental *mass balance equations* are

$$\begin{pmatrix} 1 & 1 & 1 & n_{\mathrm{C}A} & n_{\mathrm{C}D} & n_{\mathrm{C}G} \\ n_{\mathrm{H}X} & n_{\mathrm{H}V} & n_{\mathrm{H}E} & n_{\mathrm{H}A} & n_{\mathrm{H}D} & n_{\mathrm{H}G} \\ n_{\mathrm{O}X} & n_{\mathrm{O}V} & n_{\mathrm{O}E} & n_{\mathrm{O}A} & n_{\mathrm{O}D} & n_{\mathrm{O}G} \\ n_{\mathrm{N}X} & n_{\mathrm{N}V} & n_{\mathrm{N}E} & n_{\mathrm{N}A} & n_{\mathrm{N}D} & n_{\mathrm{N}G} \\ \vdots & \vdots & \vdots & \vdots & \vdots & \vdots \end{pmatrix} \begin{pmatrix} J_X \\ J_V \\ J_E \\ J_A \\ J_D \\ J_G \end{pmatrix} = \begin{pmatrix} 0 \\ 0 \\ 0 \\ 0 \\ \vdots \end{pmatrix}, \tag{2}$$

where $n_{\mathrm{C}c} = 1$ for the combined products, $c \in \{A, D, G\}$, because carbon containing products, like $\mathrm{CO_2}$, are always produced. The chemical indices of other elements can be positive or negative. For instance, the chemical indices of the element oxygen, $n_{\mathrm{O}c}$, is negative in the combined product associated with growth when there is a net consumption of O in the growth process. Notice that each new element comes with a corresponding balance equation.

Besides mass, M_c, $c \in \{V, E\}$, the two chemical compounds that constitute the individual, possess energy $\tilde{\mu}_c M_c$, where $\tilde{\mu}_c$ is the chemical potential of the compound. Besides mass fluxes J_c, $c \in \{X, A, D, G\}$ we have energy fluxes $\tilde{\mu}_c J_c$ that are carried with the materials exchanged with the environment. The mass fluxes J_c, $c \in \{X, V, E, A, D, G\}$ are

related to the energy fluxes $p_{\mathcal{P}}$, $\mathcal{P} \in \{\mathcal{A}, \mathcal{D}, \mathcal{G}\}$ by the following constitutive relationships

$$\begin{pmatrix} J_X \\ J_V \\ J_E \\ J_A \\ J_D \\ J_G \end{pmatrix} = \begin{pmatrix} -\eta_{X\mathcal{A}} & 0 & 0 \\ 0 & 0 & \eta_{V\mathcal{G}} \\ \eta_{E\mathcal{A}} & \eta_{E\mathcal{D}} & \eta_{E\mathcal{G}} \\ \eta_{A\mathcal{A}} & 0 & 0 \\ 0 & \eta_{D\mathcal{D}} & 0 \\ 0 & 0 & \eta_{G\mathcal{G}} \end{pmatrix} \begin{pmatrix} p_{\mathcal{A}} \\ p_{\mathcal{D}} \\ p_{\mathcal{G}} \end{pmatrix} , \tag{3}$$

where $\eta_{c\mathcal{P}}$ denotes the mass flux per energy flux for chemical compound c and process $\mathcal{P}$. The $\eta_{c\mathcal{P}}$'s serve as model parameters that couple energy and mass fluxes.

The energy fluxes $p_{\mathcal{P}}$, $\mathcal{P} \in \{\mathcal{A}, \mathcal{D}, \mathcal{G}\}$ determine the process rates. They are equal to the chemical energy associated with the mass flux of the reserves. This gives the following energy flux for the reserves

$$\tilde{\mu}_E J_E = p_{\mathcal{A}} - p_{\mathcal{D}} - p_{\mathcal{G}} \ . \tag{4}$$

Together with the third row of (3) we obtain for independent processes $\eta_{E\mathcal{A}} = -\eta_{E\mathcal{D}} = -\eta_{E\mathcal{G}} = 1/\tilde{\mu}_E$.

There are constraints on the mass-energy coupling parameters introduced in (3) when the energy fluxes are independent. From (2), (4) and (3) we derive

$$\begin{pmatrix} 1 & 1 & 1 & 1 & 1 & 1 \\ n_{\mathrm{H}X} & n_{\mathrm{H}V} & n_{\mathrm{H}E} & n_{\mathrm{H}A} & n_{\mathrm{H}D} & n_{\mathrm{H}G} \\ n_{\mathrm{O}X} & n_{\mathrm{O}V} & n_{\mathrm{O}E} & n_{\mathrm{O}A} & n_{\mathrm{O}D} & n_{\mathrm{O}G} \\ n_{\mathrm{N}X} & n_{\mathrm{N}V} & n_{\mathrm{N}E} & n_{\mathrm{N}A} & n_{\mathrm{N}D} & n_{\mathrm{N}G} \\ \vdots & \vdots & \vdots & \vdots & \vdots & \vdots \end{pmatrix} \begin{pmatrix} -\eta_{X\mathcal{A}} & 0 & 0 \\ 0 & 0 & \eta_{V\mathcal{G}} \\ \tilde{\mu}_E^{-1} & -\tilde{\mu}_E^{-1} & -\tilde{\mu}_E^{-1} \\ \eta_{A\mathcal{A}} & 0 & 0 \\ 0 & \eta_{D\mathcal{D}} & 0 \\ 0 & 0 & \eta_{G\mathcal{G}} \end{pmatrix} = \begin{pmatrix} 0 & 0 & 0 \\ 0 & 0 & 0 \\ 0 & 0 & 0 \\ 0 & 0 & 0 \\ \vdots & \vdots & \vdots \end{pmatrix} . \tag{5}$$

Consequently for each chemical element $\mathrm{e} \in \{\mathrm{C}, \mathrm{H}, \mathrm{O}, \mathrm{N}, \cdots\}$ there are three constraints

$$n_{\mathrm{e}A}\eta_{A\mathcal{A}} = n_{\mathrm{e}X}\eta_{X\mathcal{A}} - n_{\mathrm{e}E}/\tilde{\mu}_E \ , \tag{6a}$$

$$n_{\mathrm{e}D}\eta_{D\mathcal{D}} = n_{\mathrm{e}E}\eta_{E\mathcal{D}} \ , \tag{6b}$$

$$n_{\mathrm{e}G}\eta_{G\mathcal{G}} = n_{\mathrm{e}E}/\tilde{\mu}_E - n_{\mathrm{e}V}\eta_{V\mathcal{G}} \ . \tag{6c}$$

The number of constraints are the number of processes (3 in our case) times the number of chemical elements involved (for instance 4). Observe that these equations are just the weighted summations of the elements in the three columns of the matrix introduced in (3). These equations formulate conservation of mass for the three processes separately.

When the parameters $\eta_{c\mathcal{P}}$ with $c \in \{X, V, E\}$ for the energy transfer and storage in the two components are known, constraints (6) determine the three mass-energy conversion parameters $\eta_{c\mathcal{P}}$ for the products $c \in \{A, D, G\}$ and the processes $\mathcal{P} \in \{\mathcal{A}, \mathcal{D}, \mathcal{G}\}$ where we used $n_{\mathrm{C}c} = 1$. For other chemical elements $\mathrm{e} \in \{\mathrm{H}, \mathrm{O}, \mathrm{N}, \cdots\}$, when the chemical composition of the food, structural and reserve components, that is $n_{\mathrm{e}c}$ with $c \in \{X, V, E\}$, are

known constraints (6) determine the chemical indices n_{ec} for the products, $c \in \{A, D, G\}$. Hence, each new element comes with a corresponding balance equation and at the same time with three new constraints.

The energy fluxes for the three processes are given by the *energy balance equations*

$$-\tilde{\mu}_X J_X = p_{\mathcal{A}} + \tilde{\mu}_A J_A + p_{T\mathcal{A}} \,, \tag{7a}$$

$$0 = p_{\mathcal{D}} - \tilde{\mu}_D J_D - p_{T\mathcal{D}} \,, \tag{7b}$$

$$\tilde{\mu}_V J_V = p_{\mathcal{G}} - \tilde{\mu}_G J_G - p_{T\mathcal{G}} \,. \tag{7c}$$

The waste thermal energy in the form of generated heat are denoted by $p_{T\mathcal{P}}$, $\mathcal{P} \in \{\mathcal{A}, \mathcal{D}, \mathcal{G}\}$. For the three exothermic processes we have $p_{T\mathcal{A}} > 0$, $p_{T\mathcal{D}} > 0$ and $p_{T\mathcal{G}} > 0$ because of *the second law of thermodynamics*. Endothermic, commonly called warm-blooded, organisms can use this internally produced heat partly for the self-regulation of their body temperature which is usually higher than the environmental temperature. There is no mass flux associated with the thermal energy exchange with the environment. Chemical energy is stored in food and the products. Summation of the four equations in (4) and (7) gives the overall energy balance equation for an individual

$$\sum_{c \in \{X,V,E,A,D,G\}} \tilde{\mu}_c J_c \;+\; \sum_{p_{\mathcal{P}} \in \{\mathcal{A},\mathcal{D},\mathcal{G}\}} p_{T\mathcal{P}} = 0 \,. \tag{8}$$

Food is taken up from the environment and digestion of this food yields assimilation energy which is added to the reserves, in other words $p_{\mathcal{A}} > 0$. In addition, the energy flux to maintenance is always positive, $p_{\mathcal{D}} > 0$. When the energy stored in the reserves is too low to pay the maintenance costs, organisms can shrink. So, the energy flux for growth $p_{\mathcal{G}}$ can be positive as well as negative.

Then (3) and (7) give the following inequalities

$$\tilde{\mu}_X \eta_{X\mathcal{A}} \geq 1 + \tilde{\mu}_A \eta_{A\mathcal{A}} \,, \tag{9a}$$

$$\tilde{\mu}_D \eta_{D\mathcal{D}} \leq 1 \,, \tag{9b}$$

$$\begin{aligned} \tilde{\mu}_V \eta_{V\mathcal{G}} &\leq 1 - \tilde{\mu}_G \eta_{G\mathcal{G}} \,, \quad \text{for} \quad p_{\mathcal{G}} \geq 0 \,, \\ \tilde{\mu}_V \eta_{V\mathcal{G}} &\geq 1 - \tilde{\mu}_G \eta_{G\mathcal{G}} \,, \quad \text{for} \quad p_{\mathcal{G}} \leq 0 \,. \end{aligned} \tag{9c}$$

In summary, the two components, structural and storage materials, constitute the individual. The biomass of the structure is denoted by M_V and the biomass of the reserves by M_E. The dynamics of the food uptake together with the state equations which describe the dynamics of the two state variables fix the three energy fluxes $p_{\mathcal{P}}$, $\mathcal{P} \in \{\mathcal{A}, \mathcal{D}, \mathcal{G}\}$. Subsequently, these energy fluxes determine all mass fluxes J_c, $c \in \{X, V, E, A, D, G\}$. Thus, on the individual level the assimilation energy flux has to be considered as a time dependent forcing function describing the interaction with the food and therefore the system is non-autonomous.

In the next section the relationships between the energy fluxes $p_{\mathcal{P}}$, $\mathcal{P} \in \{\mathcal{A}, \mathcal{D}, \mathcal{G}\}$ and the state variables M_V and M_E are formulated at the population level. In a stirred

chemostat, individuals compete for food. The individuals and the food particles in the chemostat reactor are spatially homogeneously distributed. This is used with the derivation of the model for the trophic interactions. Then the population level allows the derivation of the model which describes the dynamics of the food (substrate or a prey) via a feedback, coupled to the population dynamics.

3 Population level

In Section 3.1 we will formulate the population model for a prey population consuming one nutrient and in Section 3.2 the predator population model consuming a prey population. These population models together with nutrient–prey and prey–predator interaction terms and material exchange with the environment, will be used in Section 4 for the derivation of the model for the bi-trophic food chain.

We define a number of quantities to be compliant with the notation introduced in previous work, Table 1. Two indices are used to indicate that two levels, prey and predator, are involved. We start with the definition of the population state variables. Index i denoted the trophic level of a population. In unstructured population models described by ODEs, the state variables are considered as population averages (DeAngelis and Gross, 1992). The structural biomass density is $x_i = M_{Vi} = \sum_l M_{Vil}/V_C$, that is, the sum of the structural biomasses of all individuals, which make up the population, divided by the volume of the reactor V_C. Similarly the reserves mass density is defined by $z_i = M_{Ei} = \sum_l M_{Eil}/V_C$. A scaled energy density, denoted by e_i, will be used to describe the dynamics of the reserves. It is defined by $e_i = \sum_l M_{Eil}/(\sum_l M_{Vil}[M_{Emi}]) = z_i/(x_i[M_{Emi}])$; the sum of the energy reserves per unit biomass of all individuals divided by the maximum reserve biomass density $[M_{Emi}]$ which is a species specific parameter. All mass density fluxes are given by $J_{ci} = \sum_l J_{cil}/V_C$ with $c \in \{X, A, D, G\}$, and the energy density fluxes $p_{\mathcal{P}i} = \sum_l p_{\mathcal{P}il}/V_C$ with process-index $\mathcal{P} \in \{\mathcal{A}, \mathcal{D}, \mathcal{G}\}$. Because mass and energy fluxes are additive over all individuals the constitutive relationships (3) hold also for these density fluxes J_{ci} and $p_{\mathcal{P}i}$ at the population level.

In the trophic interactions, the consumption rate is proportional to the scaled Holling type II functional response $f_{i-1,i}(x_{i-1})$, which depends on the prey population biomass density and is defined by

$$f_{i-1,i}(x_{i-1}) = \frac{x_{i-1}}{k_{i-1,i} + x_{i-1}} \,, \tag{10}$$

where $k_{i-1,i}$ is the saturation constant. We define J_{Xmi} as the maximum value of J_{Xi} when food is abundant; $f_{i-1,i}(x_{i-1}) = 1$. The maximum food uptake rate per biomass of the population $I_{i-1,i} = J_{Xmi}/x_i$ describes the interaction of all individuals with the food. A mechanistic time budget model for the nutrient uptake yields that $I_{i-1,i}$ is the inverse of the handling time and the saturation constant $k_{i-1,i}$ equates the inverse of the handling time times the search rate.

3.1 Substrate–prey system

Food consists of one component and is called substrate. We consider two levels, the substrate denoted by index 0 and the prey population level denoted by index 1.

The energy fluxes that are consistent with a simplified DEB model (Kooijman, 2000) read

$$\begin{pmatrix} p_{\mathcal{A}1} \\ p_{\mathcal{D}1} \\ p_{\mathcal{G}1} \end{pmatrix} = \begin{pmatrix} \frac{I_{0,1} f_{0,1}(x_0)}{\eta_{X\mathcal{A}1}} \\ \frac{m_1}{\eta_{V\mathcal{G}1}} \\ \frac{\nu_{0,1} e_1 - m_1 g_1}{(e_1+g_1)\eta_{V\mathcal{G}1}} \end{pmatrix} x_1 \ , \tag{11}$$

where the density of the nutrient is denoted by $x_0(t)$. The energy fluxes are expressed in the two state variables; the biomass, x_1, the scaled reserve density, e_1 where $0 \leq e_1 \leq 1$.

The parameter m_1 is called the maintenance rate coefficient, whereby energetic costs for maintenance are proportional to the structural component while reserves do not need to be maintained. Two compound parameters, the energy conductance, $\nu_{0,1}$, and the energy investment ratio, g_1, are defined by

$$\nu_{0,1} = \frac{I_{0,1}}{\eta_{X\mathcal{A}1}\tilde{\mu}_{E1}[M_{Em1}]} \ , \quad g_1 = \frac{1}{\eta_{V\mathcal{G}1}\tilde{\mu}_{E1}[M_{Em1}]} \ . \tag{12}$$

The compound parameters $\nu_{0,1}$, m_1 and g_1, one for each of the three processes, indicated in (1), are expressed in parameters of the individual level. Observe that by the introduction of these compound parameters a reduction of the number of parameters is achieved.

The expressions of the mass fluxes at the population level J_{E1} and J_{V1}, (3) can be used with (11) to derive the state equations for the dynamics of the scaled reserve mass and structural biomass of the population

$$\frac{de_1}{dt} = \nu_{0,1}\big(f_{0,1}(x_0) - e_1\big) \ , \tag{13}$$

$$\frac{dx_1}{dt} = \big(\frac{\nu_{0,1} e_1 - m_1 g_1}{e_1 + g_1}\big) x_1 \ . \tag{14}$$

These state equations describe the intrinsic dynamics of the populations with two state variables. In (Kooijman, 2000) these equations were the starting point for the modelling of the dynamics of the population. Here the energy fluxes given in (11) are chosen as the starting point, so that the state equations (13) and (14) are the outcome. There are three independent processes and two state variables, $x_1(t)$ and $e_1(t)$. However, the food abundance $x_0(t)$ serves as an extra state variable which makes independency of the three processes possible.

The mass fluxes involved in the substrate and products read

$$J_{X1} = -\eta_{X\mathcal{A}1} p_{\mathcal{A}1} = -I_{0,1} f_{0,1}(x_0) x_1 \ , \tag{15}$$

$$\begin{aligned}\sum_{c\in\{A,D,G\}} J_{c1} =& \Big(\big(1 - \frac{1}{\tilde{\mu}_{E1}\eta_{X\mathcal{A}1}}\big) I_{0,1} f_{0,1} + \frac{m_1}{\tilde{\mu}_{E1}\eta_{V\mathcal{G}1}} + \big(\frac{\nu_{0,1}e_1 - m_1 g_1}{e_1 + g_1}\big)\big(\frac{1}{\tilde{\mu}_{E1}\eta_{V\mathcal{G}1}} - 1\big)\Big) x_1 \\ =& \Big(\big(I_{0,1} - \frac{\nu_{0,1}}{g_1}\frac{1}{\tilde{\mu}_{E1}\eta_{V\mathcal{G}1}}\big) f_{0,1} + \frac{m_1}{\tilde{\mu}_{E1}\eta_{V\mathcal{G}1}} + \big(\frac{\nu_{0,1}e_1 - m_1 g_1}{e_1 + g_1}\big)\big(\frac{1}{\tilde{\mu}_{E1}\eta_{V\mathcal{G}1}} - 1\big)\Big) x_1 \ ,\end{aligned} \tag{16}$$

where we used (3,6,11) and the fact that $n_{Cc} = 1$ for $c \in \{X, V, E, A, D, G\}$. Expression (15) will be used for the description of the dynamics of the substrate. To compare this expression (16) with those obtained below with the top-down modelling approach, we do not simplify this expression using (12).

3.2 Prey–predator system

The prey population at trophic level 1 consists of two components. The predator population at trophic level 2, extracts energy from the structural component, x_1, and the reserve component, e_1. There are now two metabolic pathways to assimilate these two different nutrient sources. The growth and maintenance processes are unaltered. The four chemical transformation processes are

$$\begin{aligned} &X_{XV} \xrightarrow{\mathcal{AV},\nu} X_E + X_{AV} \ , \\ &X_{XE} \xrightarrow{\mathcal{AE},\nu} X_E + X_{AE} \ , \end{aligned} \qquad X_E \xrightarrow{\mathcal{D},m} X_D \ , \quad X_E \xrightarrow{\mathcal{G},g} X_V + X_G \ . \tag{17}$$

The uptake process is again modelled using the Holling type II functional response for the structural biomass of the prey. We assume that the storage materials are digested faster than the structural materials. The ingestion rate for the structural component of the prey is the same as for the digestion of the single structural component

$$J_{XV2} = -I_{1,2} f_{1,2}(x_1) x_2 \ , \tag{18}$$

where the scaled functional response $f_{1,2}$ is again defined by (10). Simultaneously with this structural component reserve materials are ingested. Therefore we have

$$\begin{aligned} J_{X2} = J_{XV2} + J_{XE2} &= -(1 + \frac{z_1}{x_1}) I_{1,2} f_{1,2}(x_1) x_2 \\ &= -(1 + e_1[M_{Em1}]) I_{1,2} f_{1,2}(x_1) x_2 \ . \end{aligned} \tag{19}$$

This leads to the following relationship between the mass fluxes and the energy fluxes for

the predator population

$$\begin{pmatrix} J_{XV2} \\ J_{XE2} \\ J_{V2} \\ J_{E2} \\ J_{AV2} \\ J_{AE2} \\ J_{D2} \\ J_{G2} \end{pmatrix} = \begin{pmatrix} -\eta_{XV\mathcal{A}\mathcal{V}2} & 0 & 0 & 0 \\ 0 & -\eta_{XE\mathcal{A}\mathcal{E}2} & 0 & 0 \\ 0 & 0 & 0 & \eta_{V\mathcal{G}2} \\ \eta_{E\mathcal{A}\mathcal{V}2} & \eta_{E\mathcal{A}\mathcal{E}2} & -\eta_{E\mathcal{D}2} & -\eta_{E\mathcal{G}2} \\ \eta_{AV\mathcal{A}\mathcal{V}2} & 0 & 0 & 0 \\ 0 & \eta_{AE\mathcal{A}\mathcal{E}2} & 0 & 0 \\ 0 & 0 & \eta_{D\mathcal{D}2} & 0 \\ 0 & 0 & 0 & \eta_{G\mathcal{G}2} \end{pmatrix} \begin{pmatrix} p_{\mathcal{A}\mathcal{V}2} \\ p_{\mathcal{A}\mathcal{E}2} \\ p_{\mathcal{D}2} \\ p_{\mathcal{G}2} \end{pmatrix} . \tag{20}$$

The energy fluxes read now

$$\begin{pmatrix} p_{\mathcal{A}\mathcal{V}2} \\ p_{\mathcal{A}\mathcal{E}2} \\ p_{\mathcal{D}2} \\ p_{\mathcal{G}2} \end{pmatrix} = \begin{pmatrix} \frac{I_{1,2}f_{1,2}(x_1)}{\eta_{XV\mathcal{A}\mathcal{V}2}} \\ \frac{I_{1,2}f_{1,2}(x_1)e_1[M_{Em1}]}{\eta_{XE\mathcal{A}\mathcal{E}2}} \\ \frac{m_2}{\eta_{V\mathcal{G}2}} \\ \frac{\nu_{1,2}e_2 - m_2 g_2}{(e_2+g_2)\eta_{V\mathcal{G}2}} \end{pmatrix} x_2 \ , \tag{21}$$

For the assimilation energy flux $p_{\mathcal{A}2}$ there is input from the two components, thus

$$p_{\mathcal{A}2} = p_{\mathcal{A}\mathcal{V}2} + p_{\mathcal{A}\mathcal{E}2} = (1 + \rho e_1/g_1)\frac{I_{1,2}f_{1,2}(x_1)x_2}{\eta_{XV\mathcal{A}\mathcal{V}2}} \ , \tag{22}$$

where g_1 is defined in (12) and ρ is a dimensionless constant defined by

$$\rho \stackrel{\text{def}}{=} \frac{\eta_{XV\mathcal{A}\mathcal{V}2}}{\eta_{XE\mathcal{A}\mathcal{E}2}\tilde{\mu}_{E1}\eta_{V\mathcal{G}1}} \ . \tag{23}$$

The expressions for the energy fluxes for the other two possesses, $p_{\mathcal{D}2}$ and $p_{\mathcal{G}2}$ are similar to those for the substrate–prey interaction (compare (1) with (17)). The maximum ingestion rate is now given by $I_{1,2} = J_{XVm2}/x_2$ such that $J_{XV2} = J_{XVm2}f_{1,2}$. The energy conductance, $\nu_{1,2}$ and the energy investment ratio g_2 are defined as

$$\nu_{1,2} = \frac{I_{1,2}(1+\rho/g_1)}{\tilde{\mu}_{E2}\eta_{XV\mathcal{A}\mathcal{V}2}[M_{Em2}]} \ , \quad g_2 = \frac{1}{\tilde{\mu}_{E2}\eta_{V\mathcal{G}2}[M_{Em2}]} \ . \tag{24}$$

Equation (14) for the growth remains the same. The constitutive relationship can be derived from (20) where $\nu_{1,2}$ is defined in (24), and reads now

$$\frac{de_2}{dt} = \nu_{1,2}\big(\frac{g_1 + \rho e_1}{g_1 + \rho}f_{1,2}(x_1) - e_2\big) \ . \tag{25}$$

When $\rho = 0$ the reserves of the prey individuals are not digested. For $\rho = \infty$ the predator digests only the reserves.

Because the assimilation fluxes for the two components are independent we have two constraints

$$\eta_{AV\mathcal{A}\mathcal{V}2} = \eta_{XV\mathcal{A}\mathcal{V}2} - 1/\tilde{\mu}_{E2} \ , \tag{26a}$$

$$\eta_{AE\mathcal{A}\mathcal{E}2} = \eta_{XE\mathcal{A}\mathcal{E}2} - 1/\tilde{\mu}_{E2} \ , \tag{26b}$$

where carbon is the chemical element. The sum of the mass fluxes belonging to the products, J_{c2}, $c \in \{A, D, G\}$, reads

$$\begin{aligned}\sum_{c\in\{A,D,G\}} J_{c2} =& \left(\big(1 + \frac{e_1}{g_1}\frac{1}{\tilde{\mu}_{E1}\eta_{V\mathcal{G}1}}\big) I_{1,2} - \big(\frac{\nu_{1,2}}{g_2}\frac{1}{\tilde{\mu}_{E2}\eta_{V\mathcal{G}2}}\big)\frac{g_1 + \rho e_1}{g_1 + \rho} \right) f_{1,2} x_2 \\ &+ \left(\frac{m_2}{\tilde{\mu}_{E2}\eta_{V\mathcal{G}2}} + \big(\frac{\nu_{1,2}e_2 - m_2 g_2}{e_2 + g_2}\big)\big(\frac{1}{\tilde{\mu}_{E2}\eta_{V\mathcal{G}2}} - 1\big) \right) x_2 \ ,\end{aligned} \tag{27}$$

where $\nu_{1,2}$ and g_2 are given in (24).

This completes the formulation of the model for a population feeding on a single component substrate or a two-component prey population. In the next section these population models are used to model a community in the chemostat environment.

4 Community level

In Section 4.1 we follow the bottom-up approach to derive the model for the bi-trophic food chain. The bi-trophic food chain consists of substrate, the prey and predator population. The model for the community is formed by the population models derived in the previous sections together with the model for the trophic interaction and the material exchange with the environment. In the top-down modelling approach elaborated in Section 4.2, we start with the system of state equations derived in Section 4.1. The state equations are analysed with respect to conservation laws. This approach illustrates that although product formation and heat production connected with growth is in principle possible, it is zero in the model when shrinkage is allowed.

4.1 Bottom-up approach

The chemostat is a well stirred vessel with time-invariant inflow of the substrate with density x_r, and time-invariant outflow with dilution rate D. The model reads

$$\frac{dx_0}{dt} = (x_r - x_0)D - I_{0,1}x_1 f_{0,1}(x_0) \ , \tag{28a}$$

$$\frac{de_1}{dt} = \nu_{0,1}\big(f_{0,1}(x_0) - e_1\big) \ , \tag{28b}$$

$$\frac{dx_1}{dt} = \big(\frac{\nu_{0,1}e_1 - m_1 g_1}{e_1 + g_1} - D\big)x_1 - I_{1,2}x_2 f_{1,2}(x_1) \ , \tag{28c}$$

$$\frac{de_2}{dt} = \nu_{1,2}\big(\frac{g_1 + \rho e_1}{g_1 + \rho} f_{1,2}(x_1) - e_2\big) \ , \tag{28d}$$

$$\frac{dx_2}{dt} = \big(\frac{\nu_{1,2}e_2 - m_2 g_2}{e_2 + g_2} - D\big)x_2 \ , \tag{28e}$$

where the scaled functional response $f_{i-1,i}$, $i = 1, 2$ is defined in (10). Notice that $0 \leq e_i(t) \leq 1$, $t > 0$ when $0 \leq e_i(0) \leq 1$, $i = 1, 2$.

We summarize the biological interpretations, especially the trophic interaction terms. The last term on the right-hand sides in (28a and 28c, represents the depletion rate due to predation. The consumption rate of substrate/prey is proportional to the prey/predator structural biomass density, where the proportionality parameter $I_{i-1,i}$, $i = 1, 2$ is the maximum ingestion rate. The first term on the right-hand sides in (28c, 28e) is the growth term, which is proportional to structural biomass density. Finally, there are terms due to washout, Dx_i, for all trophic levels. For the predator this is the only source of depletion. Equations (28b) and (28d) are constitutive relationships which state that the reserves biomass density dynamics follow food dynamics via a first order process. As a result (28b) and (28d) are not mass balance equations and there is no washout term.

Since modelling is done from a individual perspective all parameters, including the parameter ρ, have a meaning at this level of organization. Thus ρ in (28d) can be the ρ defined in (23).

Let q_i denote the mass densities in the chemostat of the products formed by trophic level i and these products leave the reactor via the outlet with the dilution D rate (this needs not to be true for vaporous products which leave the reactor at a different rate). Then

$$\frac{dq_i}{dt} = \sum_{c \in \{A,D,G\}} J_{ci} - Dq_i \ , \quad i = 1, 2 \ . \tag{29}$$

The mass of the two components inside the individuals and the products outside the individuals in the reactor, expressed in C-moles, can be defined as

$$K(t) = x_0(t) + \sum_{i=1}^{2} \big(x_i(t) + z_i(t) + q_i(t)\big) \ . \tag{30}$$

For this total mass it can be shown that the following equation holds

$$\frac{dK}{dt} = -\big(K(t) - x_r\big)D \ . \tag{31}$$

This is just the mass balance equation for the entire community including the substrate and products under chemostat conditions. In equilibrium we have $\lim_{t\to\infty} K(t) = x_r$. This equation states that the amount of supplied substrate Dx_r equals the net amount of substrate, biomass and products $DK(t)$ that leave the reactor, both per unit of time.

4.2 Top-down approach

Starting point is now the state equations (28) for the bi-trophic food chain in the chemostat. Since modelling is done from a community perspective all parameters, including the parameter ρ, have a meaning at this level of organization. In (Hanegraaf et al., 2000) two rates for the assimilation of the two components of the prey separately, are introduced. For the structural component the assimilation rate reads $g_1\nu_{1,2}/(g_1+\rho)$ and for the storage material $\rho\nu_{1,2}/(g_1+\rho)$, so that the sum equals $\nu_{1,2}$.

After some formula manipulation we obtain

$$\frac{dx_0}{dt} = (x_r - x_0)D - I_{0,1}f_{0,1}x_1 \ , \tag{32a}$$

$$\frac{d(1+\frac{e_1}{g_1})x_1}{dt} = \big(\frac{\nu_{0,1}}{g_1}f_{0,1} - m_1\big)x_1 - Dx_1(1+\frac{e_1}{g_1}) - I_{1,2}f_{1,2}x_2(1+\frac{e_1}{g_1}) \ , \tag{32b}$$

$$\frac{d(1+\frac{e_2}{g_2})x_2}{dt} = \big(\frac{\nu_{1,2}}{g_2}\frac{g_1+\rho e_1}{g_1+\rho}f_{1,2} - m_2\big)x_2 - Dx_2(1+\frac{e_2}{g_2}) \ . \tag{32c}$$

The dissipative mass densities p_i, one for each trophic level, are now defined by

$$\frac{dp_1}{dt} = \big(I_{0,1} - \frac{\nu_{0,1}}{g_1}\big)f_{0,1}x_1 + m_1x_1 - Dp_1 \ , \tag{33a}$$

$$\frac{dp_2}{dt} = \big(I_{1,2}(1+\frac{e_1}{g_1}) - \frac{\nu_{1,2}}{g_2}\frac{g_1+\rho e_1}{g_1+\rho}\big)f_{1,2}x_2 + m_2x_2 - Dp_2 \ . \tag{33b}$$

The last term of (32b) and (32c), which hold true also when $\rho = 0$, shows that we could have used $1+\rho e_1/g_1$ in (28d). We introduced $(g_1+\rho e_1)/(g_1+\rho)$ in order to ensure that the maximum value of the assimilation rate is independent of g_1. Furthermore, with (28d) we have now the property $0 \le e_2(t) \le 1$, $t > 0$ when $0 \le e_2(0) \le 1$ where we used (28b) to show that this feature holds for e_1.

For the function $H(t)$

$$H(t) = x_0(t) + \sum_{i=1}^{2}\left(\big(1+\frac{e_i(t)}{g_i}\big)x_i(t) + p_i(t)\right) \ , \tag{34}$$

ODE (31) holds and the solution reads

$$H(t) = x_r + \big(H(0) - x_r\big)\ \exp\{-Dt\}\ . \tag{35}$$

In an earlier paper (Kooi et al., 1999) we used this result to show boundedness of the food chain solution; an important feature of nonlinear dynamic systems.

The dissipative masses at each trophic level are the sum of two terms, namely one term is proportional to $f_{i-1,i}x_i$ connected with the assimilation energy flux, $p_{\mathcal{A}i}$, and one term is proportional to x_i connected with the dissipating energy flux, $p_{\mathcal{D}i}$. Contrary to (16) and (27) there is no term proportional to the growth rate in (33a) and (33b). This is only possible when $\eta_{V\mathcal{G}i}\tilde{\mu}_{Ei} = 1$ for all trophic levels.

When shrinkage of structure is allowed, as it is the case in system (28), this expression $\eta_{V\mathcal{G}i}\tilde{\mu}_{Ei} = 1$ can be derived from the energy balance equation (7c) and inequalities (9c) in the following way. In case of shrinking, all terms in (7c) changes sign. The heat production term in (7c) can not change sign as this would indicate heat consumption. Therefore $p_{T\mathcal{G}i} = 0$. In (Kooijman et al., 1999) shrinkage occurred during the transient dynamics towards a stable equilibrium and we let the product flux became negative, see Fig. 3(b) in that paper. However, this would mean that the inequalities (9c) become an equality $\tilde{\mu}_{Vi}\eta_{V\mathcal{G}i} = 1 - \tilde{\mu}_{Gi}\eta_{G\mathcal{G}i}$. This forms an additional constraint on the parameter values, in addition to the constraints (6c) for each element taken into account. These constraints can be satisfied only when $\eta_{G\mathcal{G}i} = 0$, $i = 1, 2$. Because $n_{\mathrm{e}Gi}\eta_{G\mathcal{G}i} = 0$, for all elements e and $\tilde{\mu}_{Ei}\eta_{V\mathcal{G}i} = 1$, constraint (6c) gives $n_{\mathrm{e}Ei} = n_{\mathrm{e}Vi}$. Hence, the chemical composition of the structural and reserve material is the same and consequently $\tilde{\mu}_{Vi} = \tilde{\mu}_{Ei}$. Hence, there is no product formation by the growth process, therefore in (1) and (17) we have

$$X_E \overset{\mathcal{G},g}{\rightleftharpoons} X_V\ .$$

Constraints on the parameters $\tilde{\mu}_{Ei}$ and $\eta_{V\mathcal{G}i}$ are not part of the system of state equations (28). Hence, the state equations do not determine the mathematical formulation completely when chemical compounds are taken into account.

Thus, the $\eta_{V\mathcal{G}i}\tilde{\mu}_{Ei} = 1$ case obtained in this section by formal mathematical manipulations starting with the state equations (28), is not just a special case: it is a reasonable formulation when shrinkage of the individuals is allowed. We have $p_i = q_i$ and $e_i(t)/g_i = z_i(t)$ where $g_i = 1/[M_{Emi}]$ and as a result $H(t)$ defined in (34) is identical with $K(t)$ defined in (30) and hence (35) describes the dynamics of the total mass in the reactor.

5 Related one-component models

In this section we describe related one-component models using our notation given in Table 1.

The chemostat model system (28) presented in the previous section is an individual-based model because modelling is done from the individual perspective. Let us compare

individual-based population models with *population-based population models*, where the parameters are defined on the individuals and population level, respectively. First, we consider the Marr-Pirt chemostat model that is obtained as a limiting case of the system (28), with $g_i = \infty$, $\nu_{i-1,i} = \infty$, so that $\nu_{i-1,i}/g_i = \mu_{i-1,i}$. For $\rho = 0$ the Marr-Pirt chemostat model reads

$$\frac{dx_0}{dt} = (x_r - x_0)D - I_{0,1}f_{0,1}x_1 \ , \tag{36a}$$

$$\frac{dx_1}{dt} = \mu_{0,1}f_{0,1}x_1 - D_1x_1 - I_{1,2}f_{1,2}x_2 \ , \tag{36b}$$

$$\frac{dx_2}{dt} = \mu_{1,2}f_{1,2}x_2 - D_2x_2 \ , \tag{36c}$$

where the functional response $f_{i-1,i}$, $i = 1, 2$, is again defined in (10). When furthermore in system (36) $m_i = 0$, $i = 1, 2$ or $D_1 = D_2 = D$, the system becomes Monod's model (Monod, 1942). A conservation principle is used in (Smith and Waltman, 1994) to show that for the study of the asymptotic behaviour, it is sufficient to consider a reduced system of only two ODEs instead of the three ODEs (36).

In another limiting case for system (28), namely with no maintenance costs, $m_i = 0$, $i = 1, 2$ and $\rho = 0$, the model is mathematically equivalent with the Droop model (Droop, 1973). The interpretation of the biomass component is the same, but that of the second component differs. In the Droop model it is internal nutrient density while in the DEB model the fate of the reserves is followed in terms of energy and mass.

The chemostat is the most commonly used system for ecological studies for aquatic habitats where nutrients are growth rate limiting. The Rosenzweig-MacArthur model (Rosenzweig and MacArthur, 1963; De Feo and Rinaldi, 1997; Gragnani et al., 1998) is often used for general theoretical analysis of ecosystem dynamics. In this population-based population model the abiotic nutrient is not modelled explicitly, the prey grows logistically in absence of the predator. The model reads

$$\frac{dx_1}{dt} = \big(r(1 - \frac{x_1}{K})\big)x_1 - I_{1,2}f_{1,2}x_2 \ , \tag{37a}$$

$$\frac{dx_2}{dt} = \mu_{1,2}f_{1,2}x_2 - D_2x_2 \ , \tag{37b}$$

where r is the intrinsic growth rate and K the carrying capacity. The interpretation of the depletion rate D_2 may be mortality rate, emigration rate or harvesting rate.

Hsu et al. (1978) showed that if there exists an asymptotically stable interior equilibrium, then it is also globally stable and Cheng (1981) proved that if such an equilibrium is unstable, then it possesses a unique globally asymptotically stable limit cycle.

In (Kooi et al., 1998b) we compared the two formulations (36) and (37). We found that if resources are explicitly taken into account, the use of the logistic equation in combination with predation, as in the Rosenzweig-MacArthur model, violates the conservation of mass.

6 Bifurcation diagrams

Bifurcation analysis provides information about the long-term dynamic behaviour of non-linear dynamic systems; the asymptotic stability of equilibria, periodic orbits and chaotic attractors. The structural stability of the dynamic systems is studied with respect to so-called free or bifurcation parameters, (Guckenheimer and Holmes, 1985; Kuznetsov, 1995). If a point, periodic or chaotic attractor changes character or disappears completely under slight adjustment of a free parameter, the system is structurally unstable. The point in the parameter space where this happens is called a bifurcation point.

Bifurcation diagrams were calculated using the software packages, AUTO (Doedel et al., 1997) and LOCBIF (Khibnik et al., 1993). The parameter values used are based on those given in (Nisbet et al., 1983) for a microbial food chain. These values for the maximum population growth rate $\mu_{i-1,i}$, the yield $y_{i-1,i} = \mu_{i-1,i}/I_{i-1,i}$ and the saturation constant $k_{i-1,i}$ are listed in Table 2. Observe that the masses are given in mg and that C-molar weights can be used as conversion factors between C-moles and mg. In (Cunningham and Nisbet, 1983), the parameters were estimated in using the Monod model ($m_i = 0$ and $g_i = \infty$, $\nu_{i-1,i} = \infty$ so that $\nu_{i-1,i}/g_i = \mu_{i-1,i}$). The additional values for the maintenance rate coefficient, m_i, and the energy investment ratio, g_i, are from (Kooi et al., 1998a; Kooi et al., 1999). By using the parameter ρ we have invariant maximum growth rates for each trophic level, see (25). This implies that the total maximum energy rate extracted from the structural and reserve components of the prey in (28d) with $f_{1,2} = 1$ and $e_1 = 1$, is fixed because $\nu_{1,2}$ is taken as an invariant parameter.

In Figure 2 we show the bifurcation diagram for the bi-trophic substrate–prey–predator food chain in the chemostat for $\rho = 0$. The two bifurcation parameters are the dilution rate D and the substrate density x_r in the reservoir. There are three biologically important regions separated by a transcritical bifurcation curve denoted by $TC_{e,2}$ and a Hopf bifurcation curve denoted by H_2. There is a region where the predator goes to extinction, a region with a point attractor which is a stable equilibrium, and one with a non-point attractor leading to oscillatory behaviour. At the transcritical bifurcation curves $TC_{e,i}$ invasion by population i through a boundary equilibrium occurs and at the Hopf bifurcation curve H_2 the bi-trophic food chain becomes unstable; it marks the origin of a stable limit cycle. Close to the Hopf bifurcation with relative large values for both bifurcation parameters there is a flip bifurcation F. A period doubling route leads to chaotic behaviour in a region enclosed by this curve F.

The growth rates denoted by $\mathcal{M}_{i-1,i}$ are defined by

$$\mathcal{M}_{i-1,i}(e_i(t)) \stackrel{\text{def}}{=} \frac{\nu_{i-1,i} e_i(t) - m_i g_i}{e_i(t) + g_i} , \quad i = 1, 2 . \tag{38}$$

Thus the individual shrinks when $\mathcal{M}_{i-1,i}(e_i(t)) < 0$ or $e_i(t) < 0.05$, as the maintenance rate coefficient m_i is chosen to be 5% of the maximum growth rate $\mu_{i-1,i} = \nu_{i-1,i}/g_i$ with $i = 1, 2$. In equilibrium we have $\mathcal{M}_{1,2} = D > 0$ for the predator population. For the prey population $\mathcal{M}_{0,1} > D > 0$ because of the extra removal term due to predation. The curve denoted by K_2 in the region with stable limit cycles gives the D, x_r-values for which at

least one of the growth rates in (38) is zero during a part of the cycle. On curve K_2 the minimum value of $e_i(t) = 0.05$, with $i = 1$ or $i = 2$, $0 \leq t \leq T_0$, where T_0 is the period of the cycle. That is, at that time t the growth rate of the prey or predator population is zero: $\mathcal{M}_{i-1,i}(e_i(t)) = 0$ with $i = 1, 2$.

Figure 3 gives a one-parameter bifurcation diagram for the equilibrium values of the predator x_2. We also plotted the extreme values (local maximum and minimum) of x_2 for the non-point attractor. In case the attractor is not a point attractor, integration is performed for a fixed time without examination of the results in order to get rid of the transients. The extreme value of the biomass of the predator calculated after this fixed time is shown as a dot in the diagram.

Extreme oscillations are found immediately after their origin at a Hopf bifurcation for high x_r-values and low or high D-values. This agrees with the result that there is shrinkage during the cycle in a large part of the bifurcation diagram shown in Figure 2 (at the right-hand side of curve K_2).

Figure 4 is an enlarged detail of Figure 3 with the minimum values for x_2 close to the Hopf bifurcation curve H_2. The rotated two-parameter bifurcation diagram Figure 2 for $280 \leq x_r \leq 300$ is plotted at the top of Figure 4. The curve K_2 intersects the $x_r = 300$ line three times. This is explained as follows. Figure 4 shows that in a region in the interval between the flip bifurcation points F there is a stable period-2 limit cycle where the minimum growth rate becomes negative. The minimum growth rate is positive again in the region around the flip bifurcation with the lowest D value. For D-values below this bifurcation point F, the minimum of x_2 decreases rapidly again and the minimum growth rate during a cycle becomes negative at the intersection with the curve K_2. The minimum growth rate during a stable limit cycle remains negative until the D-value is close to the Hopf bifurcation denoted by H_2 in Figure 3.

Figure 5 is also an enlarged detail of Figure 3 with the same D value range as Figure 4 but now the peak values of x_2 are plotted. The dynamics becomes chaotic via a route of period doubling bifurcations for D-values immediately below the Hopf bifurcation point. Observe that the cascade of period doubling occurs in a very small parameter value range for D; in Figure 3 the chaotic behaviour is hardly visible. This explains why we overlooked this phenomenon in (Kooi et al., 1999, Figure 1) where we showed this two-parameter bifurcation diagram.

7 Discussion

Predator–prey interaction is simple when each trophic level consist of two different types of biomasses without mass-energy coupling. In that case each component of the prey is (partly) added to an identical component of the predator. For instance, in the model described in (Hallam et al., 1990), the prey's lipid component can be added to the predator's lipid component. In this paper the model proposed in (Kooijman, 2000; Kooijman et al., 1999) is analysed, and mass-energy coupling is taken into account. In this case, it is not correct to add the structural biomass and reserves of the prey to the structural biomass

and reserves of the predator, respectively. Both the structure and the reserves of the prey are degraded and the extracted energy is added to the reserve pool of the predator.

In (Kooijman et al., 1999) mineral compounds; carbon dioxide, water, oxygen and nitrogen waste are distinguished from organic products. This is necessary when mineral fluxes are the subject of theoretical study or when parameters are estimated from mineral flux data. Here we constructed a more parsimonious model by adding all products and non-limiting nutrients in each independent process. We showed that one compound product per process is sufficient for a complete description. Notice that the number of state variables per population in our food chain is two, and there are three or four independent processes. This is due to the trophic interactions which couple the state equations at different levels, the last terms in (28a) and (28c).

The status of the mass fluxes of the food and the products differ in this paper. The food inflow plays a role in the trophic interaction, while the products formed at a trophic level are not consumed by organisms at other trophic levels and the ODEs for the products (29) or (33) are uncoupled from the state equations (32). Therefore the products can be calculated *a posteriori* using the solutions of the state equations.

For a chemostat system the in- and outflow rates of the mass is prescribed, but not the heat exchange with the environment. Therefore the energy balance equations are incorporated in the state equations as inequality constraints (9). When the chemical potentials $\tilde{\mu}_c$, $c \in \{X, A, D, G\}$ are known, the heat production fluxes can be calculated *a posteriori* with the energy balance equations (7) where the energy fluxes are calculated with (11).

In earlier papers (Kooi et al., 1998a; Kooi et al., 1999; Kooijman et al., 1999) the predator digests only the structural components of the prey. The system of state equations for the limiting case with $\rho = 0$ does not reduce to the system in earlier our work. In this paper it is assumed that there is an additional metabolic pathway to digest the reserves of the prey next to that for prey structure. This model choice means that the maximum assimilation rate of the predator organisms is based on the two components (24), even when the reserves of the prey are empty.

In Section 3.2 we implicitly assumed that the assimilation rate of the reserve materials is relatively fast with respect to the structural materials. However, when shrinkage is allowed we showed that the chemical composition of both components is the identical. So, when shrinkage is allowed it is implicitly assumed that the carriers can distinguish these identical components and that the two carriers and metabolic pathways work in parallel.

In a stable equilibrium the growth term is always nonnegative. However, for transients (Kooijman et al., 1999), or with periodic or chaotic attractors (in this paper) the growth term can become negative during specific periods. In other words, shrinkage of structure occurs, whereby recovered energy from structure is used to pay maintenance costs. So, the growth process can be reversed in our model formulation. As a consequence, there can be no overhead costs for the growth process when shrinkage is allowed, and products are formed in the assimilation and maintenance process only. It is the introduction of maintenance that causes modelling difficulties in the individual-based modelling approach as we shall discuss in the next paragraphs.

In (36c) of the Marr-Pirt model, the depletion rate D_2 is the sum of two rates; the

dilution rate, D, and the maintenance rate, m_2. Mathematically, in the population-based Rosenzweig-MacArthur model the time evolution of the predator is described by (37b) which equates (36c). However, now the depletion rate D_2 is the rate at which biomass diminishes. Thus, the biological interpretation of the depletion rate D_2 differs. In both models we have always $\mu_{1,2} f_{1,2}(x_1) > 0$ since $x_1 > 0$. However, in the individual-based population model, the Marr-Pirt model, there is shrinkage of the individual organisms when $\mu_{1,2} f_{1,2}(x_1) - m_2 < 0$ while still $\mu_{1,2} f_{1,2}(x_1) > 0$. Thus, contrary to the Rosenzweig-MacArthur model shrinkage can occur in the individual-based Marr-Pirt model. In summary, whether we have additional constraints on the underlying biochemical reactions, depends on the biological interpretation of the depletion rate parameter in these mathematically equivalent models.

This means that we have constraints on the biochemical reactions in the DEB model (28), just as in Marr-Pirt which is a limiting case of the DEB model. In the Droop model and the Monod model there are no maintenance costs, $m_i = 0$, $i = 1, 2$. In these models shrinkage of the individual organisms does not occur and no additional assumptions are necessary in order to obey the second law of thermodynamics. However, models without maintenance are less realistic.

Thus, it becomes crucial how the two state variables in the population model x_i and e_i are defined in terms of variables for the individuals. For instance, when all individuals have identical x_i and e_i, death caused by insufficient reserves introduces an unrealistic aspect, as all individuals die instantaneously when maintenance cannot be payed. The predator goes extinct in the region at the right-hand side of the curve K_2 in the bifurcation diagram shown in Figure 2.

In our individual-based approach the population state variables are obtained by summation over all individuals belonging to the population. Equations (13) and (25) show that for two individuals with initially different energy densities these densities become asymptotically equal. Therefore regarding the asymptotic dynamic behaviour, in our definition of the energy density at the population level no additional assumption are made. However, it is still impossible to distinguish between the individuals and therefore all individuals can only die together. Consequently, when shrinkage of structure is allowed, we have to make model choices for the case that the reserve density is insufficient to pay for maintenance.

One choice is to assume that the growth process is very efficient, that is, there is neither heat production nor product formation associated with growth. Then the predator does not go extinct, even at the right-hand side of the curve K_2 in Figure 2. Shrinkage is possible without violation of the the second law of thermodynamics while system (28) remains valid.

In (Kooijman, 2000) maintenance is modelled as the sum of somatic and maturity maintenance. Death by starvation occurs when the available energy is less than somatic maintenance costs. Now until extinction of the population, shrinkage is possible without violation of the the second law of thermodynamics.

An other choice is to model reversed growth explicitly by the introduction of a parameter which stands for the rate at which energy is liberated by shrinkage of the structure. The rate of shrinkage is then greater than the rate which follows from system (28) in order to gain extra energy for heat production and product formation, besides the energy used for

maintenance. This is, however, not an easy solution from an analysis and computational point of view. A discrete event occurs at the instant the energy density becomes insufficient to pay maintenance costs: $\mathcal{M}_{i-1,i}(e_i(t)) = 0$ for $i = 1$ or $i = 2$. Continuity conditions have to be formulated to couple the ODEs that are valid before and after the event, and the asymptotic dynamic behaviour in the region at the right-hand side of curve K_2 has to be analysed and computed anew. Modelling reversed growth explicitly is beyond the scope of this paper.

An alternative is a *physiologically structured population* formalism (PSP), in mathematical terms described by PDE instead of an ODE. In a PSP model formulation the individuals need not be identical because their physiological states are different. When food becomes scarce some individuals will die, leaving more food for survivors. In (Kooi and Kooijman, 1999) this modelling approach was used to describe the dynamics of a rotifer population consuming algae in a chemostat, where during a transient behaviour the reserves were insufficient to pay maintenance.

The consequences of the digestion of reserves on the dynamic behaviour of the bi-trophic food chain are small for moderate values of ρ in combination with large values of g_1, see (22) where $g_1 = 80$ and $e_1 \leq 1$. In a forthcoming paper we will investigate the consequences of the digestion of reserves for a tri-trophic food chain where a top-predator consumes the predator with $g_2 = 1$.

For the parameter values given in Table 2 the Marr-Pirt population models under chemostat conditions no chaotic behaviour was found, (Kooi et al., 1998a). However, with other parameter values this one component population model does show chaotic behaviour similar to that presented in this paper for the two-component model. The Rosenzweig-MacArthur model for a predator-prey system cannot show chaotic dynamics (the dimension of the autonomous continuous-time system equals 2). This holds also for the one component Monod model, but the one component Marr-Pirt chemostat model possesses chaotic (the dimension of the autonomous continuous-time system equals 3) behaviour.

8 Conclusions

We demonstrated how a biochemical modelling approach can be used to derive the state equations for the description of the dynamics of a food chain of heterotrophic organisms in the chemostat. In this paper we used a simple version of the DEB model. However, the approach is also valid when other population models with multiple components are used to formulate the relationship between the mass and energy fluxes.

The modelling approach also applies for other types of communities and other environments. Here we discussed heterotrophs in the chemostat environment as an example. Autotrophs capture solar energy and transform this energy into chemical energy by photosynthesis. This type of energy exchange with the environment is without an accompanying mass exchange as in the case of waste heat generation. In this way the derived population state equations connected by equations for trophic interactions and mass and energy exchange with the environment, form a theoretical framework for modelling ecosystems.

In a bottom-up modelling approach, an individual model is used to derive the population model. This population model together with the trophic interaction model is used to derive the community model. Often simplifying assumptions are made to make the model tractable. Here we propose the use of a top-down modelling approach to evaluate the resulting model, for instance, to check conservation laws for the whole system. This approach can reveal hidden assumptions made with the transition from individual to the community level. In (Kooi et al., 1998b) we showed that some food chain models studied in the literature do not obey mass conservation laws over the entire system, that is, nutrients included. In this paper the top-down approach reveals that the implicit assumption that shrinkage of structure is allowed means that the growth process has to be 100% efficient. On the other hand, the bottom-up modelling approach provides a mechanistic interpretation of the parameter ρ defined in (23) and used in (28d).

With one component population models where the prey-population grows logistically, as in the Rosenzweig-MacArthur model, the asymptotic dynamics for a bi-trophic microbial food chain in the chemostat is a stable equilibrium or a stable limit cycle. Chaos is found for forced bi-trophic microbial food chains in a chemostat with forcing in the form of a periodic inflow of substrate (Kot et al., 1992; Pavlou and Kevrekidis, 1992). With the DEB model, the state of each population is described by two state variables. Here we found that for this two-component model, chaotic behaviour of the bi-trophic microbial food chain in the chemostat occurs even when the reserves of the prey populations is not digested by the predator population. In addition to the one-component Marr-Pirt model, when other values for the vital parameters are used, show chaotic long-term dynamics behaviour, while the one-component Monod model does not. This shows that explicit modelling of the nutrients together with modelling of maintenance makes complex dynamic behaviour possible.

Acknowledgements

This research is supported by grant number 805.39.751 of the Netherlands Technology Foundation (STW), and is coordinated by the Council of Earth and Life Sciences (ALW).

References

Cheng, K.-S. (1981). Uniqueness of a limit cycle for predator-prey system. *SIAM J. Math. Anal.* **12**, 541–548.

Cunningham, A. and R. M. Nisbet (1983). Transients and oscillations in continuous culture. In M. J. Bazin, (ed.) *Mathematics in Microbiology*, pp. 77–103. London: Academic Press.

De Feo, O. and S. Rinaldi (1997). Yield and dynamics of tritrophic food chains. *The American Naturalist* **150**, 328–345.

DeAngelis, D. L. and L. J. Gross (1992). Preface. In D. L. DeAngelis and L. J. Gross, (eds.) *Individuals-based Models and Approaches in Ecology*, pp. xv–xviii. New York: Chapman & Hall.

Doedel, E. J., A. R. Champneys, T. F. Fairgrieve, Y. A. Kuznetsov, B. Sandstede and X. Wang (1997). Auto 97: Continuation and bifurcation software for ordinary differential equations. Technical report, Concordia University, Montreal, Canada.

Droop, M. R. (1973). Some thoughts in nutrient limitation in algae. *J. Phycol.* **9**, 264–272.

Gragnani, A., O. De Feo and S. Rinaldi (1998). Food chains in the chemostat: relationships between mean yield and complex dynamics. *Bulletin of Mathematical Biology* **60**, 703–719.

Guckenheimer, J. and P. Holmes (1985). *Nonlinear Oscillations, Dynamical Systems and Bifurcations of Vector Fields*, volume 42 of *Applied Mathematical Sciences*. New York: Springer-Verlag, 2 edition.

Hallam, T. G., R. R. Lassiter, J. Li and L. A. Suarez (1990). Modelling individuals employing an integrated energy response: Application to *Daphnia*. *Ecology* **71**, 938–954.

Hanegraaf, P. P. F., B. W. Kooi and S. A. L. M. Kooijman (2000). The role of intracellular components in food chain dynamics. *Comptes rendus de l'Academie des science series III-Sciences de la vie-life* **323**, 99–111.

Herbert, D. (1958). Some principles of continuous culture. In G. Tunevall, (ed.) *Recent progress in Microbiology*, pp. 381–396. Oxford, England: Blackwell.

Hsu, S. B., S. P. Hubbell and P. Waltman (1978). Competing predators. *SIAM J. Appl. Math.* **35**, 617–625.

Khibnik, A. I., Y. A. Kuznetsov, V. V. Levitin and E. V. Nikolaev (1993). Continuation techniques and interactive software for bifurcation analysis of ODEs and iterated maps. *Physica D* **62**, 360–371.

Kooi, B. W., M. P. Boer and S. A. L. M. Kooijman (1998a). Consequences of population models on the dynamics of food chains. *Mathematical Biosciences* **153**, 99–124.

Kooi, B. W., M. P. Boer and S. A. L. M. Kooijman (1998b). On the use of the logistic equation in food chains. *Bulletin of Mathematical Biology* **60**, 231–246.

Kooi, B. W., M. P. Boer and S. A. L. M. Kooijman (1999). Resistance of a food chain to invasion by a top predator. *Mathematical Biosciences* **157**, 217–236.

Kooi, B. W. and S. A. L. M. Kooijman (1999). Discrete event versus continuous approach to reproduction in structured population dynamics. *Theoretical Population Biology* **56**, 91–105.

Kooijman, S. A. L. M. (2000). *Dynamic Energy and Mass Budgets in Biological Systems*. Cambridge: Cambridge University Press.

Kooijman, S. A. L. M., B. W. Kooi and T. G. Hallam (1999). The application of mass and energy conservation laws in physiologically structured population models of heterotrophic organisms. *Journal of Theoretical Biology* **197**, 371–392.

Kot, M., G. S. Sayler and T. W. Schultz (1992). Complex dynamics in a model microbial system. *Bulletin of Mathematical Biology* **54**, 619–648.

Kuznetsov, Y. A. (1995). *Elements of Applied Bifurcation Theory*, volume 112 of *Applied Mathematical Sciences*. New York: Springer-Verlag.

Monod, J. (1942). *Recherches sur la croissance des cultures bactériennes*. Hermann, Paris.

Nisbet, R. M., A. Cunningham and W. S. C. Gurney (1983). Endogenous metabolism and the stability of microbial prey-predator systems. *Biotechnol. Bioeng.* **25**, 301–306.

Pavlou, S. and I. Kevrekidis (1992). Microbial predation in a periodically operated chemostat: A global study of the interaction between natural and externally imposed frequencies. *Mathematical Biosciences* **108**, 1–55.

Persson, L., K. Leonardsson, A. M. de Roos, M. Gyllenberg and B. Christensen (1998). Ontogenetic scaling of foraging rates and the dynamics of a size-structured consumer-resource model. *Theoretical Population Biology* **54**, 270–293.

Pirt, S. J. (1965). The maintenance energy of bacteria in growing cultures. *Proc. Roy. Soc. London (B)* **163**, 224–231.

Polis, G. A. and K. O. Winemiller, (Eds.) (1996). *Food webs*. New York: Chapman & Hall.

Roels, J. A. (1983). *Energy and kinetics in biotechnology*. Amsterdam: Elsevier Biomedical Press.

Rosenzweig, M. L. and R. H. MacArthur (1963). Graphical representation and stability conditions of predator-prey interactions. *The American Naturalist* **97**, 209–223.

Smith, H. L. and P. Waltman (1994). *The Theory of the Chemostat*. Cambridge: Cambridge University Press.

Uchmański, J. and V. Grimm (1996). Individuals-based modelling in ecology: what makes the difference? *Trends in Ecology and Evolution* **11**, 437–441.

Table 1: Parameters and state variables; t=time, m=biomass, e=energy, V=volume of the reactor. The index i denotes the trophic level, $\mathcal{P} \in \{\mathcal{A}, \mathcal{D}, \mathcal{G}\}$ a process and $c \in \{X, V, E, A, D, G\}$ a chemical compound.

Parameter	Dimension	Interpretation
D	t^{-1}	Dilution rate
e_i	—	Reserve biomass density
g_i	—	Energy investment ratio, $\propto$ costs for growth
$I_{i-1,i}$	$\mathrm{m\ m^{-1}t^{-1}}$	Maximum food uptake rate
J_{ci}	$\mathrm{m\ V^{-1}t^{-1}}$	Mass flux density
$k_{i-1,i}$	$\mathrm{m\,V^{-1}}$	Saturation constant
m_i	t^{-1}	Maintenance rate coefficient
M_{ci}	$\mathrm{m\ V^{-1}}$	Biomass density
$[M_{Emi}]$	$\mathrm{m\,m^{-1}}$	Maximum mass reserves per structural mass
$p_{\mathcal{P}i}$	$\mathrm{e\,V^{-1}t^{-1}}$	Energy flux
p_i	$\mathrm{m\,V^{-1}}$	Dissipating mass density
q_i	$\mathrm{m\,V^{-1}}$	Product mass density
t	t	Time
x_0	$\mathrm{m\,V^{-1}}$	Substrate density
x_i	$\mathrm{m\,V^{-1}}$	Structural biomass density
x_r	$\mathrm{m\,V^{-1}}$	Substrate concentration in reservoir
$y_{i-1,i}$	$\mathrm{m\ m^{-1}}$	Maximum yield
z_i	$\mathrm{m\,V^{-1}}$	Reserve biomass density
$\eta_{c\mathcal{P}i}$	$\mathrm{m\ e^{-1}}$	Flux mass per flux energy
$\mu_{i-1,i}$	t^{-1}	Maximum population growth rate
$\tilde{\mu}_{ci}$	$\mathrm{e\ m^{-1}}$	Chemical potential
$\nu_{i-1,i}$	t^{-1}	Energy conductance, $\propto$ assimilation rate

Table 2: Parameter set for bacterium-ciliate models, after (Cunningham and Nisbet, 1983) and (Nisbet et al., 1983). The values for the new parameters m_i (equal to 5% of maximum growth rate $\mu_{i-1,i}$) and g_i are also given. The relationships $I_{i-1,i} = \mu_{i-1,i}/y_{i-1,i}$ and $\mu_{i-1,i} = \nu_{i-1,i}/g_i$ hold true for $i = 1, 2$.

Parameter	Unit	Values	
		$i = 1$	$i = 2$
$k_{i-1,i}$	$\mathrm{mg\,dm^{-3}}$	8	9
$I_{i-1,i}$	$\mathrm{h^{-1}}$	1.25	0.333
m_i	$\mathrm{h^{-1}}$	0.025	0.01
g_i	—	80.0	1.0
$\nu_{i-1,i}$	$\mathrm{h^{-1}}$	40.0	0.2
$y_{i-1,i}$	—	0.4	0.6
$\mu_{i-1,i}$	$\mathrm{h^{-1}}$	0.5	0.2

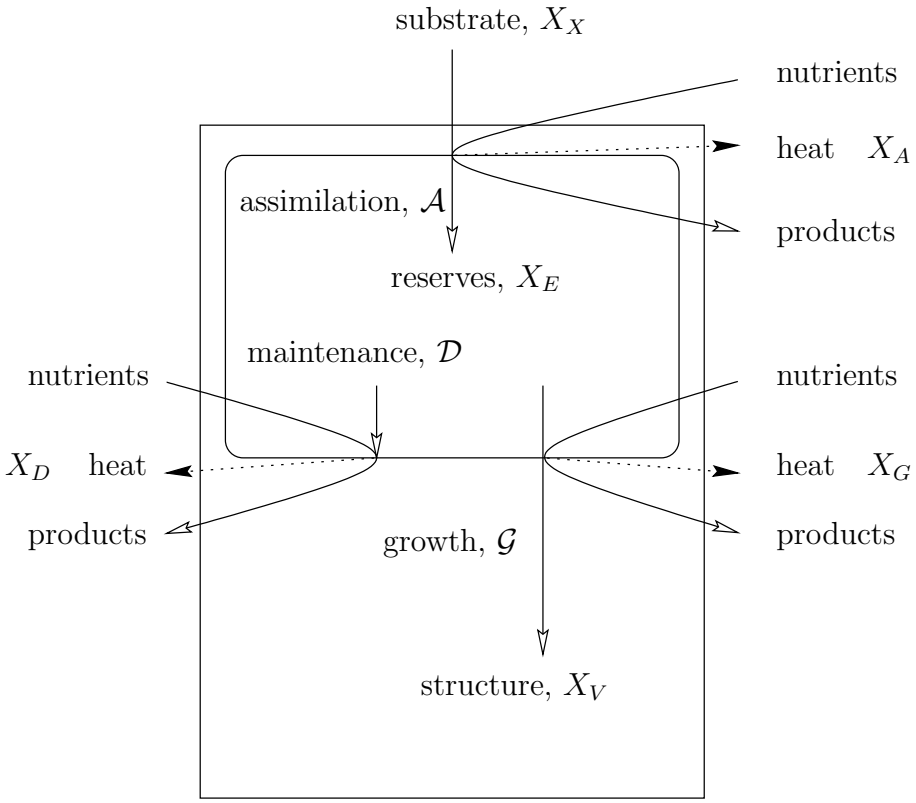

Figure 1: Mass and energy fluxes for the DEB model. There are three processes; assimilation, $\mathcal{A}$, maintenance, $\mathcal{D}$, and growth, $\mathcal{G}$. There are two components that constitute the individual; structural component, X_V, and the reserves component, X_E, and four chemical compounds that are exchanged with the environmental; substrate, (food, nutrient) X_X, and products (organic compounds like faeces and minerals: carbon dioxide, nitrogen waste) or non-limiting nutrients (oxygen, vitamin) together denoted by X_c, with $c \in \{A, D, G\}$. Waste heat is produced with each process.

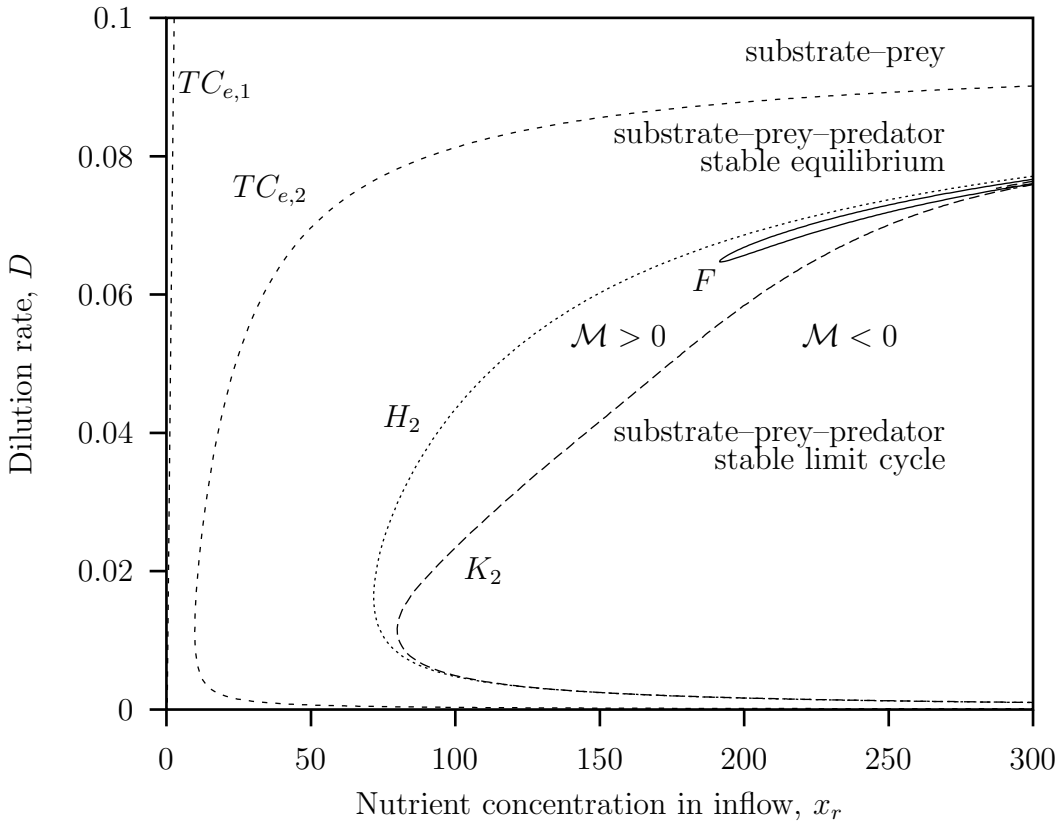

Figure 2: Bifurcation diagram for DEB model with two trophic levels: system (28) with $\rho = 0$. Values assigned to physiological parameters are listed in Table 2. The curves $TC_{e,1}$ and $TC_{e,2}$ are transcritical bifurcation curves and H_2 marks a Hopf bifurcation curve. The solid curve F indicates a flip bifurcation for limit cycles. The curve K_2 indicates where one of the population growth rates $\mathcal{M}_{i-1,i}(t)$, $i = 1, 2$ becomes zero in a distinct point in time during a limit cycle.

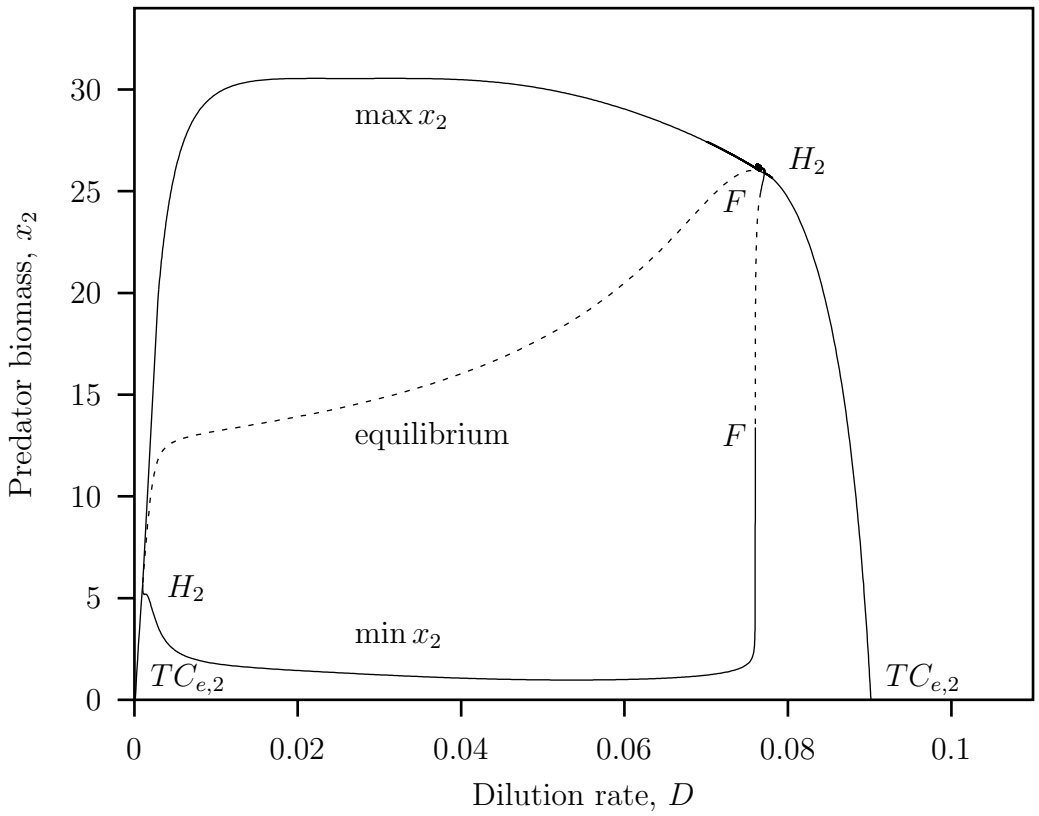

Figure 3: One-parameter bifurcation diagram with characteristic values of the predator x_2. The bifurcation parameter is the dilution rate D. The concentration in the reservoir is $x_r = 300$. Solid curves give stable equilibrium values and the minimum and minimum values of x_2 with stable period-1 limit cycles. Dashed curves give unstable versions. For a description of the symbols see Figure 2.

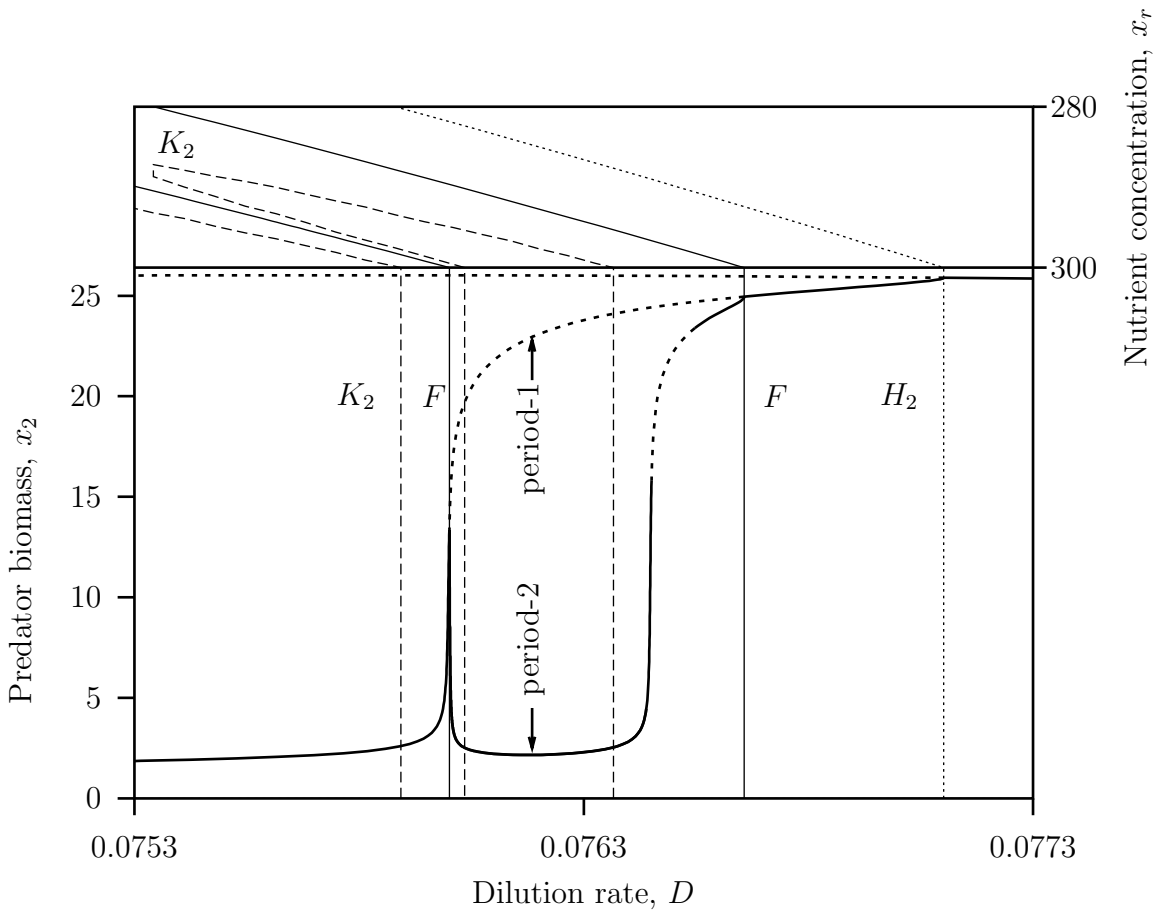

Figure 4: One-parameter bifurcation diagram with minimum values of the predator x_2. This is an enlargement of Figure 3. Solid curves give stable equilibrium values and minimum values of stable equilibrium limit cycles. Dashed curves give unstable equilibrium values or minimum values of unstable limit cycles. At the top a part of the the rotated two-parameter bifurcation diagram, Figure 2 is plotted for $280 \leq x_r \leq 300$. Bifurcation points (the dilution rates for intersection points in the two-parameter bifurcation diagram of bifurcation curves with the $x_r = 300$ line) are indicated by vertical lines.

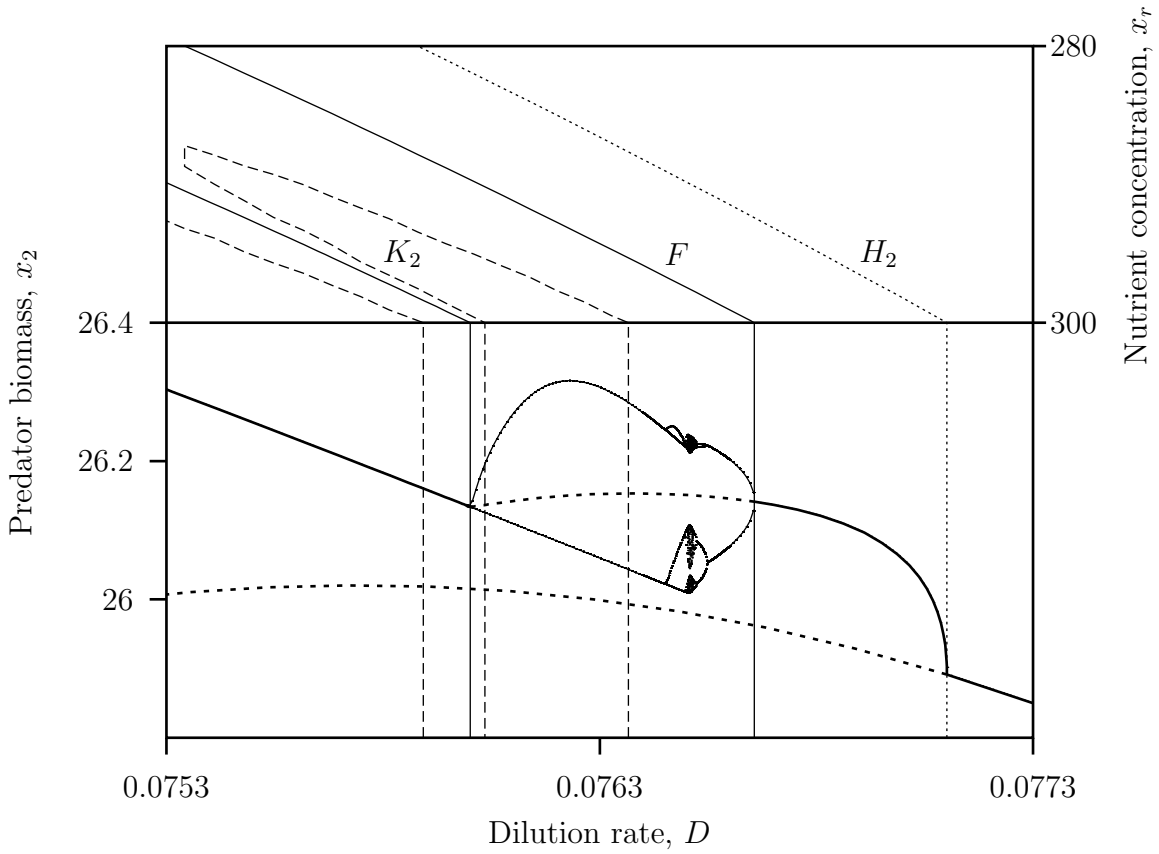

Figure 5: One-parameter bifurcation diagram with maximum values of the predator x_2. For a description of the curves and the symbols see Figure 3.